Characterization of the intermetallic G-phase in an AISI 329 duplex stainless steel

A. MATEO, L. LLANES, M. ANGLADA
Departament de Ciències dels Materials i Enginyeria Metal.lúrgica, Universitat Politècnica de Catalunya, Av. Diagonal 647, 08028 Barcelona, Spain

A. REDJAÏMIA, G. METAUER
Laboratoire de Science et Génie des Surfaces, URA-CNRS 1402 EMN/EEIGM, Parc de Saurupt, 54042 Nancy Cedex, France

Duplex austenite–ferrite stainless steels are susceptible to a variety of decomposition processes when aged within the intermediate range of temperatures (250–500 °C). One of these phenomena is the precipitation of the intermetallic G-phase. In the present investigation, the crystal structure and the chemical composition of the G-phase, precipitated in the ferritic phase of an AISI329 duplex stainless steel, is studied by electron microdiffraction and energy dispersive X-ray spectroscopy. It is determined that the space group of the G-phase is $F\frac{4}{m}\bar{3}\frac{2}{m}$ with a lattice parameter four times that of the ferritic matrix. The precipitation mechanism of the G-phase showed a synergetic relation with the ferrite decomposition in Cr-rich and Fe-rich domains. Based on the obtained results, the structural proximity of ferrite matrix and G-phase has been studied. Further analysis allows to suggest that the spinodal decomposition leads to an interdomain of a ferritic structure which is thermodynamically unstable and serves as a precursory site to the development of the G-phase by atomic position readjustments inferior to the atomic distances.

1. Introduction

Two-phase austenite–ferrite duplex stainless steels are being increasingly used as a structural material in oil, chemical and power industries [1–4]. This is mainly because their duplex microstructure allows a beneficial combination of austenitic and ferritic properties: on the one hand high strength with a desirable toughness [5, 6] and, on the other, good corrosion resistance, specially to chloride-induced stress corrosion cracking [7–9]. However, one of the main problems which limits their use is the embrittlement that they experience when exposed in the intermediate temperature range 250–500 °C [10, 11]. This embrittlement produces a considerable change in the mechanical properties under both monotonic [12, 13] and cyclic [14, 15] loading conditions.

Generally, the spinodal decomposition of ferrite into chromium-rich (α') and iron-rich (α) domains is considered to be the main cause of the above embrittlement [16, 17]. However, spinodal decomposition is not the only microstructural change which duplex steels can suffer during ageing in this temperature range. Other processes include: reactions in the ferrite (precipitation of phases such as α', G-phase, carbides and formation of austenite), reactions at ferrite–austenite boundaries (precipitation of carbides and nitrides) and reactions in the austenite (spinodal-like decomposition, sigma-phase precipitation) [17]. In this work, the crystallographic and microstructural characteristics of the referred G-phase, an intermetallic compound which usually precipitates in association with the spinodal reaction, have been studied in detail.

The G-phase is a silicide, first identified by Beattie and Ver Snyder [18] in a Fe–Ni superalloy A-286. The arbitrary name of G-phase was assigned owing to its prominent appearance at grain boundaries. It is often found in austenitic stainless steels after irradiation [19, 20]. Similarly, several investigations [21–24] have reported and dealt with G-phase precipitation during low temperature ageing in cast duplex steels of the ASME SA351 CF series. However, a complete crystallographic characterization of the intermetallic G-phase in any kind of stainless steel has not been well documented yet. Such detailed characterization is of extreme significance because it is expected to provide valuable insights into the precipitation mechanism associated with G-phase formation.

Thus, the objective of this investigation is to characterize the intermetallic G-phase precipitated within the ferrite matrix of an AISI329 duplex stainless steel as a consequence of thermal ageing. Such information is then used as a basis for studying the structural similitude between the G-phase and its corresponding ferritic matrix.

0022–2461

2. Material and experimental procedure

The studied material was an AISI329 duplex stainless steel produced by ACENOR (Spain). Two melts for this alloy were studied. Their compositions are given in Table I. The as-received materials were solution treated at 1050 °C for one hour to achieve homogeneity and to maximize the percentage of austenite, which finally was 38% for melt A and 21% for melt B. Specimens were then thermally aged in a temperature range between 275 and 475 °C for various times up to 20 000 h (2.3 years).

Thin foils were prepared following conventional transmission electron microscopy (TEM) sample preparation methods. The samples were first ground to about 20 μm thickness. Then, they were electropolished in a Struers Tenupol twin jet unit operating at 35 V potential and using a solution of 5% perchloric acid in 95% II-butoxyethanol. The characterization of crystal structures was performed by microdiffraction using a Philips CM12 transmission electron microscope operated at 120 kV. Two tilt-rotation goniometers and double-tilt stages were employed for maximizing structural information. Quantitative chemical analyses were carried out with an energy dispersive X-ray spectroscopy (EDS) system attached to a Philips CM20 scanning-transmission electron microscope. An X-ray diffractometer, equipped with a source of CoK_α radiation ($\lambda = 0.17902$ nm), was employed to determine the lattice parameters of the constitutive phases, α and γ, present in the duplex stainless steel.

3. Phase identification

TEM observations reveal that, in addition to the spinodal decomposition of the ferritic-phase, and at temperatures over 375 °C, ageing treatments lead to variable G-phase precipitation in the ferrite. The size of these particles, typically between 20 and 50 nm, depends on the ageing conditions.

At the highest temperature (475 °C) studied and for the longest ageing times, the distribution of these particles is quite homogeneous (Fig. 1) and the density of particles increases with time. At lower temperatures, and for relatively short ageing times at 475 °C, the precipitation is less dense and, often, the particles seem to nucleate and coarsen on dislocations (Fig. 2).

Two-dimensional (2D) and especially three-dimensional (3D) symmetry information, required to determine the crystal structure of G-phase precipitated as very small particles, is not present in convergent beam electron diffraction (CBED) patterns. Morniroli and Steeds [25] have shown that crystal structure characterization, in such a case, may be achieved through microdiffraction patterns obtained by focusing a nearly parallel electron beam onto a very small area of the specimen. The zone axis microdiffraction patterns thus obtained, are composed of small diameter discs grouped into ZOLZ and HOLZ (zero and high order Laue zones, respectively). From the information of these microdiffraction patterns it is possible to determine the following crystallographic features.

(a) The "net" and "ideal" symmetries which are concerned, respectively, with the position and both the position and the intensity of the reflections on the microdiffraction pattern. These symmetries are in connection with the crystal system and the point group, respectively.
(b) The shift between the ZOLZ and the FOLZ (first order Laue zone) reflection nets. This is related to the Bravais lattice.
(c) The periodicity difference between the ZOLZ and the FOLZ reflection nets. This is in connection with the presence of a glide plane.

In such a way, the crystallographic features of the G-phase were determined from the recorded microdiffraction patterns by a systematic method given in detail elsewhere [25, 26]. All these patterns show intense reflections belonging to the ferritic matrix superimposed to some of the G-phase (weaker reflections). The symmetry determination of the G-phase is not

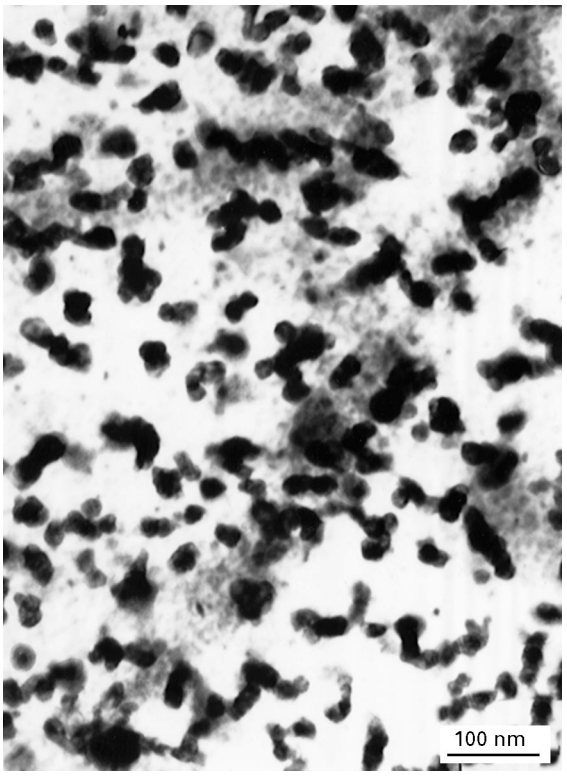

Figure 1 G-phase precipitation in a duplex steel aged at 475 °C for 15 000 h.

TABLE I Chemical composition of the AISI329 duplex stainless steels (wt %)

Heat	C	Mn	Si	Cr	Ni	Mo	N	Fe
A	0.036	1.73	0.34	24.60	5.40	1.40	0.072	Bal.
B	0.044	1.75	0.77	25.00	5.25	1.37	0.027	Bal.

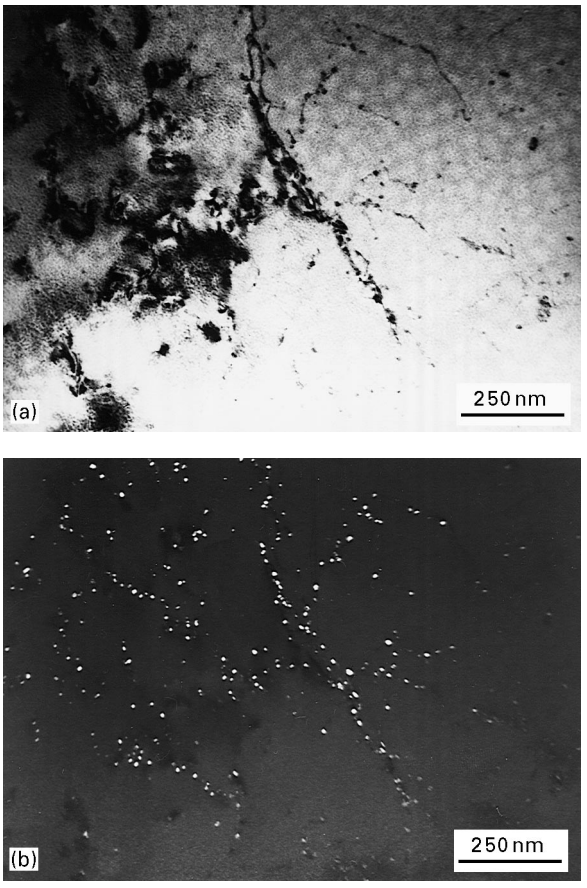

Figure 2 Preferential G-phase precipitation on dislocations. Specimen aged at 475 °C for 200 h. (a) Bright field; (b) Dark Bragg field.

altered by the presence of the ferrite. The latter has the most symmetric point group, i.e. the holosymmetric $m\bar{3}m$.

Among the investigated zone axis patterns (ZAPs) of the G-phase, it appears that the highest "net" symmetry of the ZOLZ corresponds to (4mm) and (6mm) (Fig. 3a and b). According to Tables 7 and 2 in [25], these symmetries correspond to a cubic system and are observed, respectively, along $\langle 0\,0\,1\rangle$ and $\langle 1\,1\,1\rangle$ ZAPs. Thus, from Table 5 in [25], the specific ZAPs to investigate in order to identify the Bravais lattice and glide plane are along $\langle 0\,0\,1\rangle$ and $\langle 1\,1\,0\rangle$. Unfortunately, the weakness of reflection intensities makes it difficult for the FOLZ to be observed. Usually to solve this problem, the operating voltage of the microscope is reduced so as to decrease the FOLZ radius or the specimen is cooled to liquid-nitrogen temperature to enhance the intensity of the FOLZ reflections. However, in this investigation, these two approaches were unsuccessful. To overcome this difficulty, the specimen may be slightly tilted around the zone axis until the FOLZ area appears on the pattern with stronger reflections. This experimental solution, which was previously suggested by Steeds and Vincent [27], constitutes an elegant method to carryout, with great success, the characterization of the ZOLZ/FOLZ shifts and periodicity differences to identify the Bravais lattice and the glide planes.

In so doing, on the tilted $\langle 0\,0\,1\rangle$ ZAP (Fig. 4a), two squares with sides parallel to mirrors m_1 and m_2 are drawn both in the ZOLZ and the FOLZ. In agreement with the theoretical simulations from Fig. 9d in [25], the corresponding individual partial extinction symbols, as described by Buerger [28], as either F– • • or I– • •. On the other hand, on the tilted $\langle 1\,1\,0\rangle$ ZAP (Fig. 4b), two centred rectangles with sides parallel to mirrors m_1 and m_2 are drawn both in the ZOLZ and the FOLZ. Examination of the tilted ZAP and its comparison with the theoretical one established in Fig. 9d in [25] reveals that the individual partial extinction symbol is F• • –. As there is no translation symmetry element along $\langle 1\,1\,1\rangle$ zone axis, the addition of the two individual partial extinction symbols leads to F––– partial extinction symbol. As indicated in the "International Tables for Crystallography" [29], this F––– extinction symbol may be associated with six spaces groups belonging to five point groups as summarized in Table II.

The number of the possible space groups can be restricted through the identification of the point group by means of the "ideal" ZOLZ symmetries of the $\langle 0\,0\,1\rangle$, $\langle 1\,1\,0\rangle$ and $\langle 1\,1\,1\rangle$ ZAPs (Fig. 3). These ZAPs exhibit (4mm), (2mm) and (6mm) "ideal" ZOLZ symmetries, respectively. Then, according to Table 4a in [25], the corresponding point group is $m\bar{3}m$. This leads to the unambiguous conclusion that the space group for the G-phase is $Fm\bar{3}m$, or $F\,\frac{4}{m}\,\bar{3}\,\frac{2}{m}$ in its full crystallographic notation.

4. Orientation relationship and lattice parameter

The investigated ZAPs are composed of two patterns belonging to the G-phase (weak reflections) and the ferrite (stronger reflections) (Fig. 3), and show that the G-phase adopts a cube-on-cube orientation relationship with the ferritic matrix, i.e. there is a parallelism between planes and directions with the same crystallographic indexes. These relationships, which agree with those previously reported [21, 22], may be described as:

$$(0\,0\,1)_G//(0\,0\,1)_\alpha$$

$$(1\,1\,0)_G//(1\,1\,0)_\alpha$$

$$(1\,1\,1)_G//(1\,1\,1)_\alpha$$

The construction of the stereogram (Fig. 3) common to the bcc ferritic and the fcc G-phase permits the indexation of the diffraction patterns obtained along $[0\,0\,1]$, $[0\,1\,1]$ and $[\bar{1}\,1\,1]$ with no difficulty. As a result of the corresponding calculations from these patterns, the G-phase parameter is exactly four times that of ferrite ($a_G = 4a_\alpha$). The lattice parameter of the matrix, calculated by indexing the peaks from the X-ray diffraction pattern, was found to be 0.2871 nm. Hence, the G-phase lattice parameter of the AISI 329 duplex stainless steel studied is 1.1484 nm. It is interesting to point out that such a ratio of four ($a_G = 4a_\alpha$) is in the upper range of that usually reported [20–24], from 3.8 to 4 times that of the ferrite in which the G-phase is found. Following previous results and ideas, it is suggested that differences in chemical composition result in a series of G-phases of variable lattice parameter.

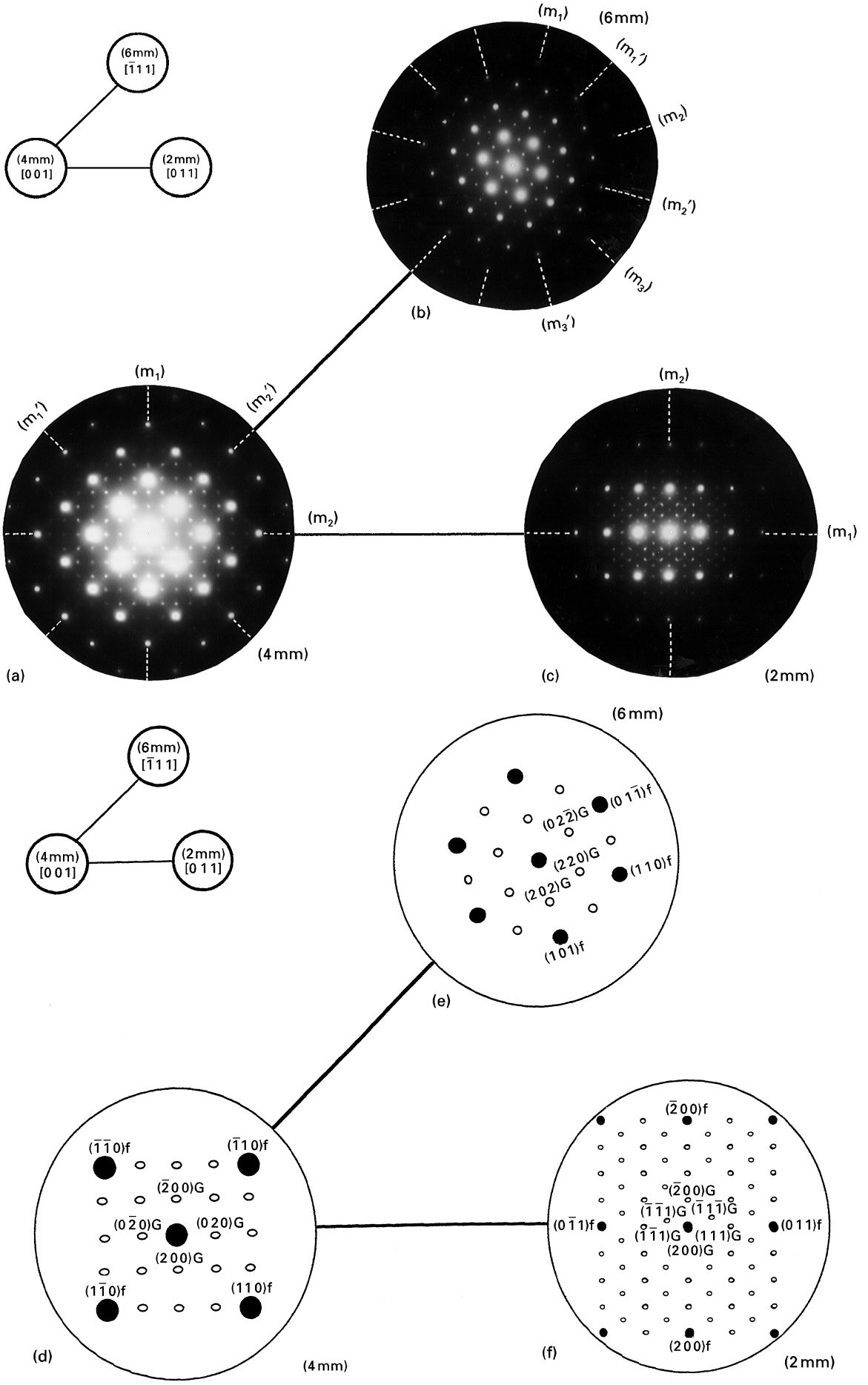

Figure 3 Microdiffraction patterns for the cubic G-phase and the ferritic matrix recorded along: (a) $[0\,0\,1]_G//[0\,0\,1]_\alpha$ zone axis, (b) $[\bar{1}\,1\,1]_G//[\bar{1}\,1\,1]_\alpha$ zone axis, (c) $[0\,1\,1]_G//[0\,1\,1]_\alpha$ zone axis, (d) indexation of pattern in (a), (e) indexation of pattern in (b), and (f) indexation of pattern in (c).

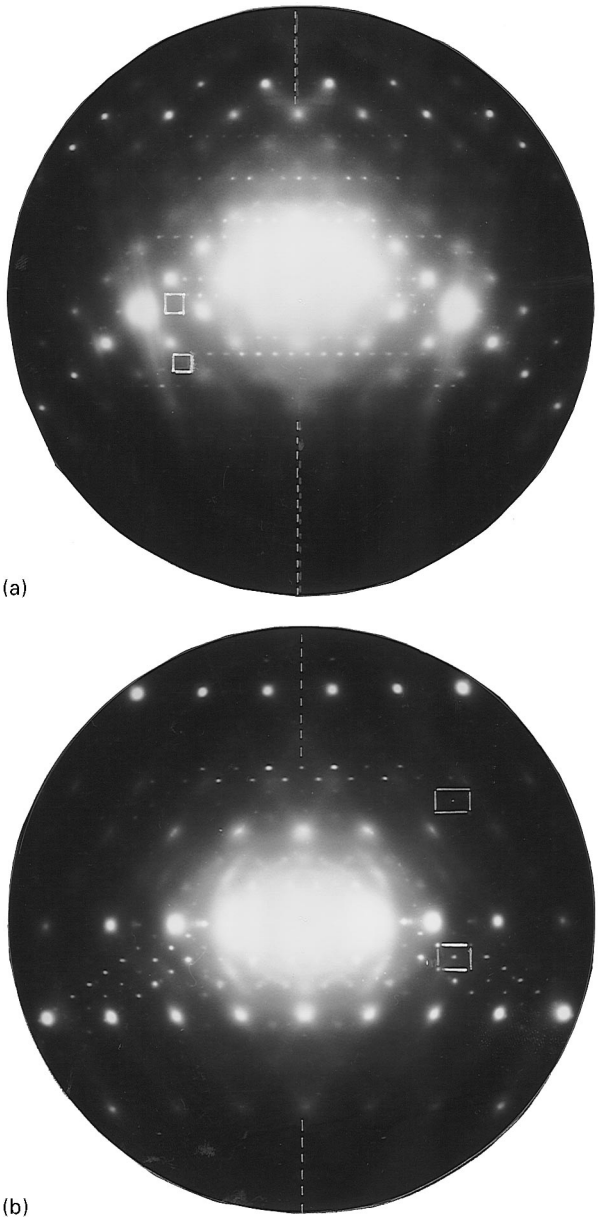

Figure 4 Tilted microdiffraction patterns recorded along: (a) ⟨0 0 1⟩; (b) ⟨1 1 0⟩.

TABLE II Space groups and point groups for extinction symbol F − − −

Extinction symbol	Space groups	Point groups
F − − −	F23	23
	$F\frac{2}{m}\bar{3}$	$\frac{2}{m}\bar{3}$
	F432	432
	$F4_132$	
	$F\bar{4}3m$	$\bar{4}3m$
	$F\frac{4}{m}\bar{3}\frac{2}{m}$	$\frac{4}{m}\bar{3}\frac{2}{m}$

5. Further considerations

It is well established that the morphology of transformation products taking place in a solid matrix is of great importance in materials science. The equilibrium shape and the habit plane, respectively, adopted and developed between the transformation products and the parent phase have been extensively investigated. Both the morphology and the variant number of precipitates, which adopt orientation relationships with the matrix, can be understood in terms of group theory as developed elsewhere [30, 31]. This approach based on the shared symmetry elements of the two point groups could be applied to explain the G-phase precipitation features. However, considering the cube-on-cube orientation relationship developed by the G-phase with the ferrite matrix, both belonging to the same point group $\frac{4}{m}\bar{3}\frac{2}{m}$, the symmetry analysis becomes trivial, leading to $\frac{4}{m}\bar{3}\frac{2}{m}$ as the common group. Similar considerations result, for the G-phase, in an index of subgrouping (the number of precipitate variants of a given orientation relationship) equal to 1. This means that for the G-phase, there is only one variant taking place in every grain of the matrix. This result is compatible with the observations in Bragg dark field, i.e. no matter which $h\,k\,l$ reflection of a zone axis is used to record an image, every G-phase particle of the observed area is illuminated (Fig. 2).

In terms of the intrinsic characteristics of the G-phase precipitation several aspects may be pointed out:

First, such G-phase precipitation appears during the spinodal decomposition of the ferrite, after an incubation time, for all ageing temperatures. Chemical composition analyses were carried out in the thinnest areas of the samples, very close to the electrochemical hole. The results obtained under these circumstances are given in Table III. They show that the weight percentage level of Fe in G-phase is inferior to that of the ferrite before the ageing treatment, and the level of Cr is higher than that of unaged ferrite and lower than that of α'. Compared with the composition obtained from the adjacent matrix, the G-phase is largely richer in Ni, Mo, Mn and Si. The diffusion of the latter elements is closely related to the precipitation of the G-phase. It must be said that G-phase formation seems to be very sensitive to the presence of Si atoms. This feature is consistent with the assumption that the incubation time for G-phase formation is associated with the low diffusion rate of silicon in the ferrite [32].

Second, the fluxes of the different elements during spinodal decomposition of the ferrite strongly support the idea already suggested [17], and here reinforced, of a synergetic effect between the G-phase formation and the spinodal decomposition. Indeed, the G-phase formation may be proposed to occur following two steps: the first one is described by the mechanism illustrated in Fig. 5: spinodal decomposition implies an enrichment of α and α', both adjacent domains of this decomposition, in Fe and Cr, respectively. Besides such fluxes, the α domain rejects Si and Mo atoms and the α' domain rejects Ni and Mn atoms. In fact, the spinodal decomposition leads to an interdomain of a ferritic structure which is very unstable thermodynamically and this serves as a precursory site for the development of the G-phase. The α/α' interdomain, enriched in alloying elements which will participate

TABLE III Chemical composition analysed by EDS on a specimen of Heat B before ageing and after being exposed at 475 °C for 4000 h

(wt %)	Fe	Cr	Ni	Mo	Mn	Si
G-phase	42.18	29.24	12.43	6.45	4.39	5.31
Ferrite matrix before ageing	66.45	25.46	4.07	1.66	1.67	0.69
Ferrite spinodally decomposed (α′)	56.94	36.09	2.48	2.16	1.11	1.21

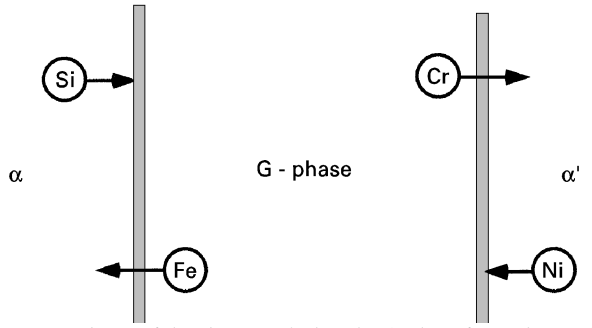

Figure 5 Fluxes of the elements during the G-phase formation and the spinodal decomposition of the ferrite.

later in the G-phase formation, would be a thermodynamically unstable ferrite. The second step corresponds to the attainment by the α/α′ interdomain of a critical chemical composition which is very close to that of the G-phase. This intermetallic compound will then precipitate under favourable conditions. The incubation time recorded for the G-phase precipitation corresponds to the length of time to reach a critical composition.

The above diffusion-related ideas may also explain the observation of dislocations as preferential precipitation sites for the G-phase. In simple terms, diffusion assistance along the dislocation core must result in an enhancement of the whole precipitation process, as suggested by Miller and Bentley [22].

Third, taking into account the experimental results on the correlation between the lattice parameters of the matrix and the G-phase, as well as their orientation relationship, together with the consideration that the G-phase is isostructural with the intermetallic compound Th_6Mn_{23} and the silicide $Ni_{16}Si_7Ti_6$ [33], the structural proximity of both phases may be further analysed. For the $Ni_{16}Si_7Ti_6$ stoichiometric compound the unit cell contains 116 atoms, which occupy, from the "International Tables for Crystallography" [29], the positions reported in Table IV. In the case of the duplex steel studied here, chemical analyses show that Ti atoms have been replaced by Cr and Mn atoms, whereas Ni has been substituted by a Fe–Ni–Mo combination. A projection of the atoms of the cell of the G-phase along the $\langle 0\,0\,1\rangle$ direction (Fig. 6), represented using commercial software (MolView, @ JM Cense), shows that it can be described as a stacking of atomic planes (A to H) which are equidistant and parallel to (1 1 0) plane. Then, it is judicious to make a comparison between the $\{1\,1\,0\}$ planes of the G-phase and the $\{1\,1\,0\}$ close-packed planes of the bcc crystals of ferrite. Although most of the atoms of the eight layers are on a plane of the cell, others are

TABLE IV Position of atoms at the unit cell of $Ni_{16}Si_7Ti_6$

Type of atom	Number of atoms (Wyckoff notation)	*X*	*Y*	*Z*
Si	4(b)	0.500	0.500	0.500
Si	24(d)	0.000	0.250	0.250
Ni	32(f)	0.378	0.378	0.378
Ni	32(f)	0.178	0.178	0.178
Ti	24(e)	0.203	0.000	0.000

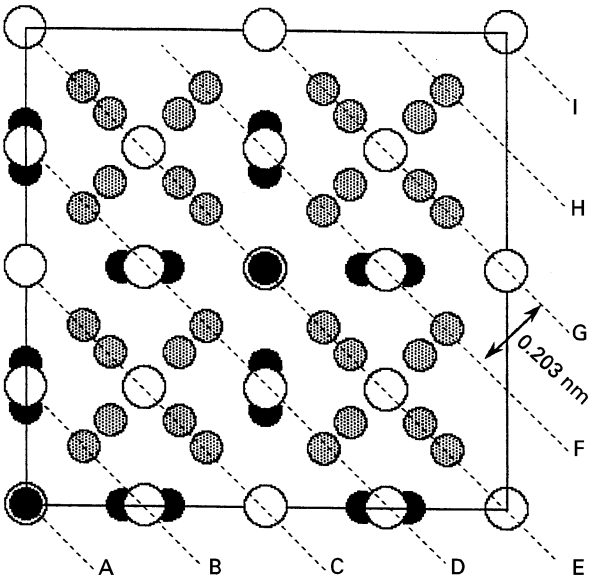

Figure 6 Projection along $\langle 0\,0\,1\rangle$ of the atoms which compose the G-phase cell: ○ Si atoms; ● Ti atoms; ◍ Ni atoms.

aside from it. In these latter cases the calculated separations are much shorter than the interatomic distances. The largest separation is smaller than 0.1 nm. Under these circumstances, the atomic distribution of the G-phase should be described as a stacking of corrugated layers.

Based on the cube-on-cube orientation relationship and the unit cell parameters, the G-phase cell can be expressed as a super-cell containing 64 ferrite unit cells. This superstructure would contain 128 atoms (2×64). However, the G-phase cell is found to hold 116 atoms. Three sets of layers may be distinguished in Fig. 6. One set includes layers A and E, and it is the least compact of the three types (Fig. 7a). Another set, represented by layers B, D, F and H (Fig. 7b), is characterized for having the same compactness as that of $\{1\,1\,0\}$ planes in ferrite. The final set, which includes layers C and G (Fig. 7c) shows an intermediate compactness between the former two. The absence of

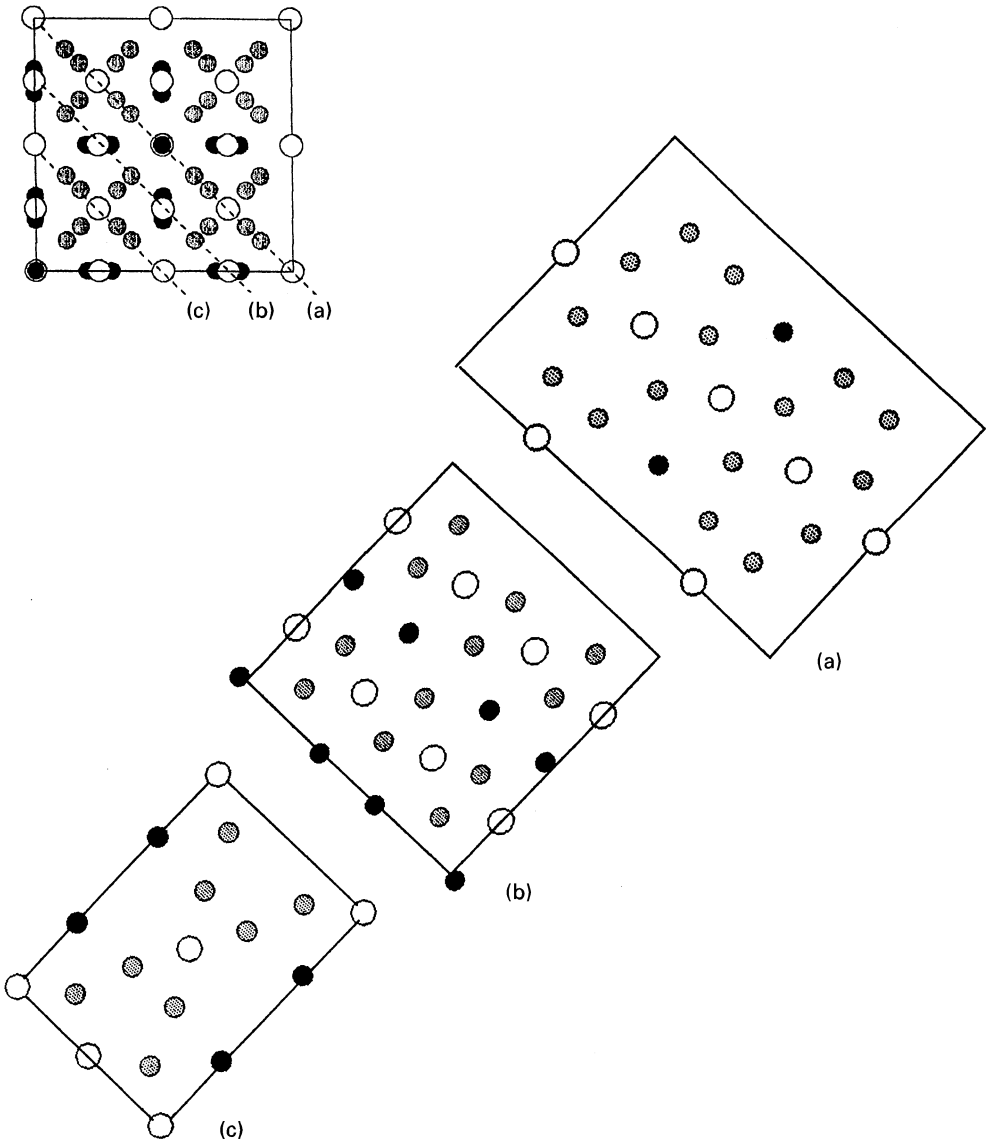

Figure 7 Schematic representation of the distribution of G-phase atoms on the layers compiled parallel to (1 1 0) plane. (a) Projection of atoms on layers A, E and I. (b) Projection of atoms on layers B, D, F and H. (c) Projection of atoms on layers C and G.

12 atoms is a direct consequence of the lack of compactness of the last two sets of layers. The superposition of the projection of G-phase atoms to the ferrite supercell along $\langle 1\,1\,0 \rangle$ direction shows the similarities between the atomic layer distribution (Fig. 8). The analysis of the similarities between the distribution of the atoms in the G-phase and in the ferritic supercell now allows us to better describe the second step within the G-phase precipitation as the unstable ferrite of the α/α' interdomain reaching its critical chemical composition and then transforming into the G-phase by atomic position readjustments. The amplitudes of these readjustments are smaller than the interatomic distances, and from the position of the atoms of G-phase and ferrite, are calculated to be:

$$\delta Ni^{\alpha} \rightarrow Ni^{G}_{(3)} = 0.0060 \text{ nm}$$

$$\delta Ni^{\alpha} \rightarrow Ni^{G}_{(4)} = 0.1052 \text{ nm}$$

$$\delta Si^{\alpha} \rightarrow Si^{G} = 0 \text{ nm}$$

$$\delta Ti^{\alpha} \rightarrow Ti^{G} = 0.0539 \text{ nm}$$

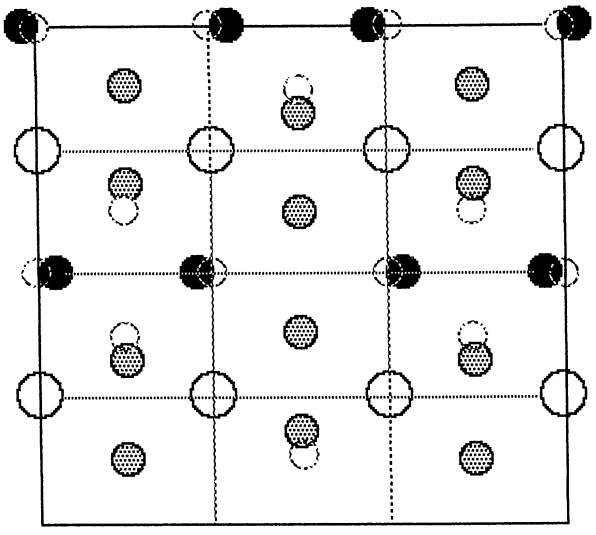

Figure 8 Schematic representation of the atomic displacements for the $\alpha \rightarrow G$ transition on the D layer. α-matrix and G-phase atoms are indicated by discontinuous and continuous marks, respectively.

6. Conclusions

The thermal ageing of duplex ($\alpha + \gamma$) stainless steels in the temperature range between 275 and 475 °C leads to a series of metallurgical transformations which mainly take place in the ferritic phase. This research work has been concentrated on the G-phase, an intermetallic compound rich in Ni and Si, precipitated within the ferritic matrix of an AISI 329 duplex stainless steel.

The characterization by electron microdiffraction determines unambiguously that the G-phase crystallizes in the fcc system, belongs to the space group $F\frac{4}{m}\bar{3}\frac{2}{m}$, and adopts a cube-on-cube orientation relationship with the ferritic matrix with a lattice parameter a_G four times a_α.

The G-phase appears, with an incubation time, after the spinodal decomposition of the ferrite. From the experimental results and literature reports the G-phase precipitation is further discussed and is suggested to occur following two steps:

1. an enrichment of the interdomains α/α' by diffusion due to the spinodal decomposition and usually assisted by matrix dislocations; and
2. once that the interdomains have reached the critical chemical composition, the G-phase precipitation takes place by atomic readjustments whose amplitude is smaller than the interatomic distances.

Acknowledgements

The authors wish to express their gratitude to ACENOR (Spain) for kindly supplying the steel used for this investigation. We thank J. Ghanbaja, Univ. H. Poincaré (Vandoeuvre-lès-Nancy) for the chemical analysis by EDS. Part of this work has been supported by the ECSC (European Coal and Steel Comission) under Contract No. 7210-MA/940. One of the authors (A.M.) wishes to thank a fellowship from the *CIRIT* (*Generalitat de Catalunya*) Ref. AIRE94/II-15.

References

1. R. M. DAVISON and J. M. REDMOND, *Mater. Performance* **29** (1990) 57.
2. H. KIESHEYER, in Proceedings of the International Conference on Stainless Steels'91, (The Iron and Steel Institute of Japan, Chiba, 1991), p. 1148.
3. D. J. A. FRUYTIER, in Proceedings of the International Conference Duplex Stainless Steels'91, Vol. 1 edited by J. Charles and S. Bernhardsson, (Les Éditions de Physique, Les Ulis, 1991) p. 497.
4. J. CHARLES, M. VERNEAU and B. BONNEFOIS, in Proceedings of the 2nd European Congress on Stainless Steels'96 (Eds. VEDh Dusseldorf, 1996) p. 97.
5. I. TAMURA and Y. TOMOTA, in Proceedings of the Symposium on Mechanical Behaviour of Materials, Vol. 2 (Japan Society of Materials Science, Kyoto, 1974) p. 105.
6. J. FOCT, N. AKDUT and G. GOTTSTEIN, *Scripta Metall. Mater.* **27** (1992) 1033.
7. N. SRIDHAR, J. KOLTS and L. H. FLASCHE, *J. Metals* **37** (1985) 31.
8. T. MAGNIN and J. M. LARDON, *Mater. Sci. Eng.* **A 104** (1988) 21.
9. S. BERNHARDSSON, J. OREDSSON and C. MARTENSON, in Proceedings of the International Conference on Duplex Stainless Steels'82, edited by R. A. Lula (ASM, Metals Park, Ohio, 1983) p. 267.
10. M. GUTTMANN, in Proceedings of the International Conference on Duplex Stainless Steels'91, Vol. 1, edited by J. Charles and S. Bernhardsson (Les Éditions de Physique, Les Ulis, 1991) p. 79.
11. L. ITURGOYEN, PhD thesis, Univ. Politècnica Catalunya, Spain (1994).
12. O. K. CHOPRA and H. M. CHUNG, in Proceedings of the 3rd International Symposium on Environmental Degradation of Materials in Nuclear Power System-Water Reactors, edited by G. J. Theus and J. R. Weeks (The Metallurgical Society, Warrendale, 1988) p. 737.
13. L. ITURGOYEN, J. ALCALÁ and M. ANGLADA, in Proceedings of the International Conference on Duplex Stainless Steels'91, Vol. 2, edited by J. Charles and S. Bernhardsson, (Les Éditions de Physique, Les Ulis, 1991) p. 757.
14. T. J. MARROW, PhD thesis, University of Cambridge, UK (1991).
15. L. LLANES, A. MATEO, L. ITURGOYEN and M. ANGLADA, *Acta Mater.* **44** (10) (1996) 3967.
16. R. LAGNEBORG, *Trans. Amer. Soc. Metals* **60** (1967) 67.
17. H. M. CHUNG, *Int. J. Pres. Ves. Piping* **50** (1992) 179.
18. H. J. BEATTIE and F. L. VER SNYDER, *Nature* **178** (1956) 208.
19. E. H. LEE, P. J. MAZIASZ and A. F. ROWCLIFFE, in "Phase Stability during Irradiation". edited by J. R. Holland, L. K. Mansur and D. I. Potter. (TMS-AIME, Warrendale, 1981) p. 191.
20. W. J. S. YANG, H. R. BRAGER and F. A. GARNER, in "Phase Stability during Irradiation", edited by J. R. Holland, L. K. Mansur and D. I. Potter (TMS-AIME, Warrendale, 1981) p. 257.
21. J. M. VITEK, S. A. DAVID, D. J. ALEXANDER, J. R. KEISER and R. K. NANSTAD, *Acta Metall. Mater.* **39** (1991) 503.
22. M. K. MILLER and J. BENTLEY, *Mater. Sci. Technol.* **6** (1990) 285.
23. J. M. VITEK, *Metall. Trans.* A **18A** (1987) 154.
24. J. J. SHIAO, C. H. TSAI, J. J. KAI and J. H. HUANG, *J. Nuclear Mater.* **217** (1994) 269.
25. J. P. MORNIROLI and J. W. STEEDS, *Ultramicroscopy* **45** (1992) 219.
26. A. REDJAÏMIA and J. P. MORNIROLI, *ibid.* **53** (1994) 305.
27. J. W. STEEDS and R. VINCENT, *J. Microsc. Spectrosc. Electron.* **8** (1983) 617.
28. M. J. BUERGER, "Elementary Crystallography" (Massachussetts Institute of Technology Press, Cambridge, 1978).
29. T. HAHN (ed.) "International Tables for Crystallography" (Reidel, Dordrecht, 1988).
30. R. PORTIER and D. GRATIAS, *J. Phys. Sup. No. 12* **43** (1982) C4-17.
31. J. W. CAHN and G. KALONJI, in Proceedings of the Conference on Solid-Solid Phase Transitions, edited by H. I. Aaronson, R. F. Sekereka, D. E. Laughlin and C. M. Waymann (Metall. Soc. AIME, Warrendale, 1982) p. 3.
32. R. J. BORG and D. Y. F. LAI, *J. Appl. Phys.* **41** 3 (1970) 5193.
33. E. HLADYSHEVSKII, P. I. KRIPYAKEVICH, YU. B. KUZMA and M. YU. TESLYUK, *Krystalographya* **6** (1961) 769.

Received 10 October 1996
and accepted 10 February 1997